



4th IASPEI / IAEE International Symposium:

Effects of Surface Geology on Seismic Motion

August 23–26, 2011 • University of California Santa Barbara

MAGNITUDE SCALING IN GROUND-MOTION PREDICTION EQUATIONS FOR RESPONSE SPECTRA FROM LARGE SUBDUCTION INTERFACE EARTHQUAKES FROM JAPAN

John X. Zhao
GNS Science
Lower Hutt
New Zealand

ABSTRACT

Magnitude-scaling rates (MSRs, the rates of increase in predicted response spectrum with increasing moment magnitude) are evaluated for three ground-motion prediction equations for response spectra from subduction interface earthquakes, including two empirical models developed for data from Japan and a model based on synthetic records generated by using a stochastic finite-fault model. MSRs vary significantly among the three models, and the difference between the two empirical models is unacceptably large. A set of 2100 strong-motion records from subduction interface events with a magnitude of 6.5 or larger from Japan, including the 11 March, 2011 magnitude 9 earthquake, were compiled. A simple attenuation model was fitted to the data and the model has a constant term for each earthquake group to represent the effect of magnitude. Three separate functions of magnitude, a linear model for events with a magnitude over 7, a bilinear model and a curved model, were then fitted to the constants and MSRs were derived from these functions. At short periods, the derived MSRs are only a fraction of those from two of the three attenuation models. At spectral periods over 0.5s, the derived MSRs are between about 1/3 and 1/2 of those of the two empirical models, but closer to those based on a set of synthetic records.

INTRODUCTION

Zhao and Lu (2011) evaluated the magnitude-scaling rate (MSR) for 5 modern ground-motion prediction equations for shallow large crustal earthquakes. They found that the MSRs of the four Next Generation Attenuation (NGA) models (Abrahamson & Silva 2008, Boore & Atkinson 2008, Campbell & Bozorgnia 2008, and Chiou & Youngs 2008) varied significantly. Zhao and Lu (2011) also showed that a model without a magnitude term fits the response spectra from 12 of the 13 large crustal earthquakes with moment magnitude M_W over 7 very well, suggesting zero magnitude scaling. They attributed zero magnitude scaling to the rapid increase in fault length and duration of strong shaking with increasing magnitude and to the reduced energy ratio (the energy contributed to the response spectra over the total energy of a strong-motion record) for records from large earthquakes. For large subduction interface earthquakes with M_W over 7, the increase in magnitude may similarly lead to an increase in duration but may not necessarily lead to a significant increase in ground-motion amplitude. The present study will investigate this aspect.

The recent $M_W=9$ earthquake (11 March 2011 Japan Time) caused devastating tsunami and human casualties. However, a large set of strong-motion records was obtained from this event, 230 records within a source distance (the closest distance to the fault rupture) of 300km and the largest horizontal peak ground acceleration (PGA) of 2.75g from a rock/stiff shallow soil site at a source distance of 70km. The PGAs from 5 records exceed 1g at a source distance over 59km. Figure 1a compares the normalized PGA (corrected to SC II site class conditions defined in Zhao et al. 2006a, using the site terms from Zhao et al. 2006b, and referred to as Z2006) with the prediction from the Z2006 model. Figure 1(b) compares the spectral accelerations at 3s spectral period with the same model. The Z2006 over-predicted the recorded ground motion by a very large factor compared with the best fit using the similar functional form to that of the Z2006. The preliminary comparison with the other attenuation models shows that the Kanno et al. (2006) (referred to as

K2006) model, the Atkinson and Boore et al. (2003) model, and the Gregor et al. (2002) (referred to as G2002) model have very similar extent of over-prediction (D. Boore 2011, personal communication).

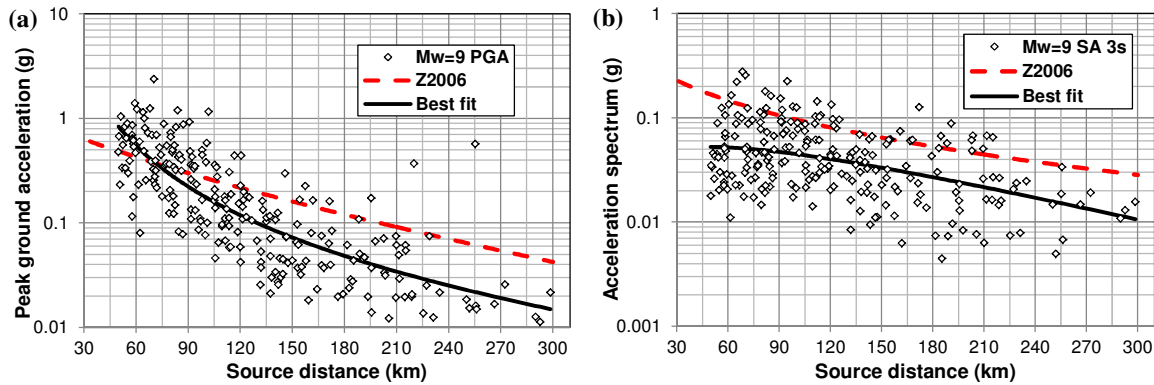


Figure 1 Comparison between the recorded spectra, the prediction by the Zhao et al. (2006a) (referred to as Z2006) model and the best model fitted to the data using the form of the Z2006 model, (a) peak ground acceleration; and (b) spectral acceleration at 3s spectral period. The PGA and spectrum were normalized to site class II, i.e. multiplied by $\exp(S_k - S_2)$ where S_k and S_2 are the site terms of the Z2006 model for the k^{th} class and the 2nd class, respectively

The over-prediction may be caused largely by magnitude scaling, as none of the datasets used in these models contains any event over 8.3. For the models that used the data from the 26 September 2003 $M_w=8.3$ earthquake in Japan, the magnitude scaling is still not well constrained. Many models have a magnitude squared term or magnitude-cubed term with a negative coefficient that enhances the magnitude scaling for earthquakes with M_w less than about 6.5 and reduces the magnitude scaling for large earthquakes. Zhao et al. (2006a) interpreted the enhanced magnitude scaling for small events at long periods as a result of the calculation of response spectra when energy associated with short-period ground motions contributes to the response spectra at long spectral period. However, the coefficient for the magnitude squared term is usually unnecessary for short spectral periods. The magnitude squared term is largely controlled by the small events, which outnumber the large events by many times. In the present study, the subduction interface events with $M_w=6.5$ or larger, including the recent $M_w=9.0$ event, will be used to assess the magnitude scaling rate (MSR) for large earthquakes without being constrained by small earthquakes.

The Z2006 model and K2006 model were both based on data from Japan, including the September 2003 $M_w=8.3$ earthquake. The K2006 model used a much larger dataset than the Z2006 model, with many events that do not have source types (tectonic locations, such as shallow crustal, subduction interface and subduction slab). The K2006 model does not have a magnitude squared term and the standard deviation for the model is much larger than that from the Z2006 model. Any differences in magnitude scaling for the two models may be a result of the functional form used in these models.

The G2002 model was developed by using the results from numerical simulation based on a stochastic finite-fault model developed by Silva et al. (1990) and calibrated by the 19 September 1985 $M_w=8.0$ Michoacan, Mexico, earthquake and the 3 March 1985 $M_w=8.0$ Valparaiso, Chile, earthquake. The magnitude scaling from this model will also be investigated. If appropriate MSRs can be derived from numerical simulation, such numerical modelling can be used to constrain the model predictions for large earthquakes, or fill in the magnitude gap among real events.

For all models, we used linear and squared or cubed magnitude terms, and magnitude-dependent geometric terms, to compute response spectra while the effects of focal depth and site terms were not included. The computed spectra were then normalized with respect to the spectrum computed for $M_w=6.5$ at source distances of 30, 60, 120, 180 and 240 km. Note that all distances are the closest distance to the fault rupture plane. The magnitude-scaling rate (MSR) is defined as the average slope of a curve in a 2-D plot for the normalized spectra in logarithm scale with respect to moment magnitude in linear scale. The effect of magnitude-dependent geometric attenuation is included.

Figure 2 shows the normalized spectra for the Z2006 model. Figure 2(a) shows that, at a 30km distance, the PGA for a magnitude 9 event is about 4.7 times that of an $M_w=6.5$ event and this ratio increases with increasing source distance. At a source distance of 240km, the PGA from an $M_w=9$ event is about 11.7 times that from an $M_w=6.5$ event. The MSRs generally decrease with increasing magnitude. This model does not have a magnitude-squared term for PGA and the reduced MSR at large magnitude is the effect of an added magnitude-dependent distance term in the geometric attenuation function. At large distances, the MSR is essentially constant. Figure 2(b) shows the normalized spectra at 0.4s. At large distances, the normalized spectra at all magnitudes are similar to the normalized PGA. At a distance of 30km, the normalized spectra are similar to the normalized PGA at a distance of 60km. The

normalized spectra at 0.4s and a distance of 60km are generally similar to those of the normalized PGA at a distance of 120km. Figure 2(c) shows the normalized spectra at 2s spectral period from the Z2006 model. The variation of MSRs is twice those at 0.4s period at all distances. Figure 2(d) shows that, at 5s, the normalized spectra at distances larger than 120km are similar to those at 2s period at the same distance, while the normalized spectra at a source distance of 80km or less are considerably smaller than those at 2s period at the same distance. Zero MSRs at 5s period occur at magnitude over 9 and at a source distance of less than 80km (the result from 80km is not shown). The linear magnitude term in the Z2006 model varies between just over 1.0 for PGA to just below 2.0 at long periods, as suggested by the slope of the normalized spectra at magnitude between 6.5 and 7.0.

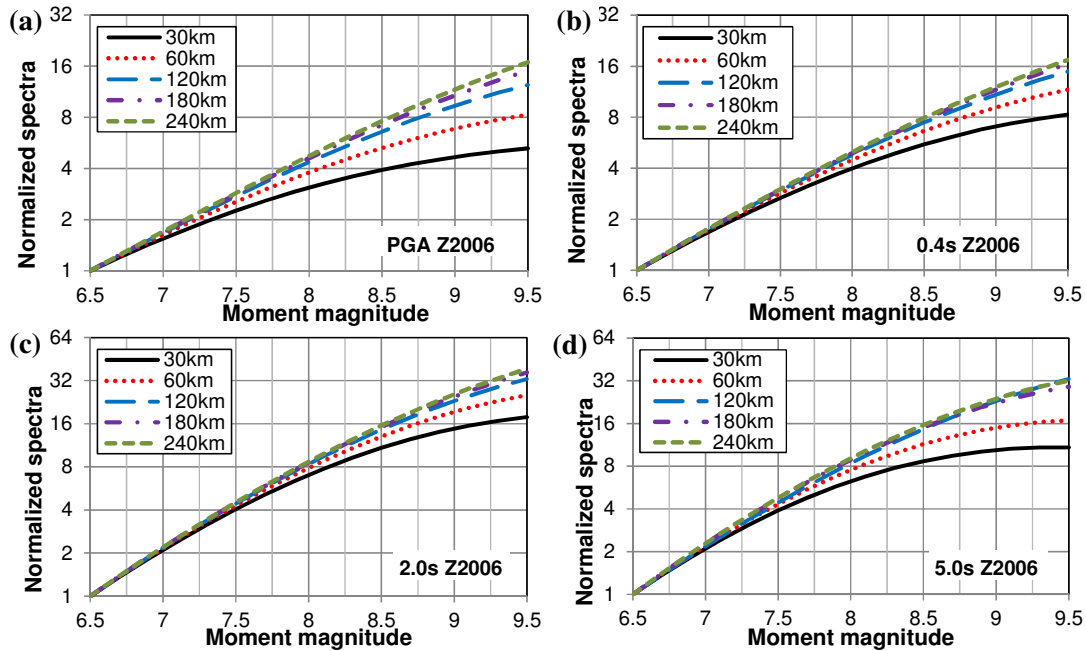


Figure 2 Normalized spectra predicted by the Zhao et al. 2006a model for (a) peak ground acceleration, (b) 0.4s, (c) 2 and (d) 5s spectral periods

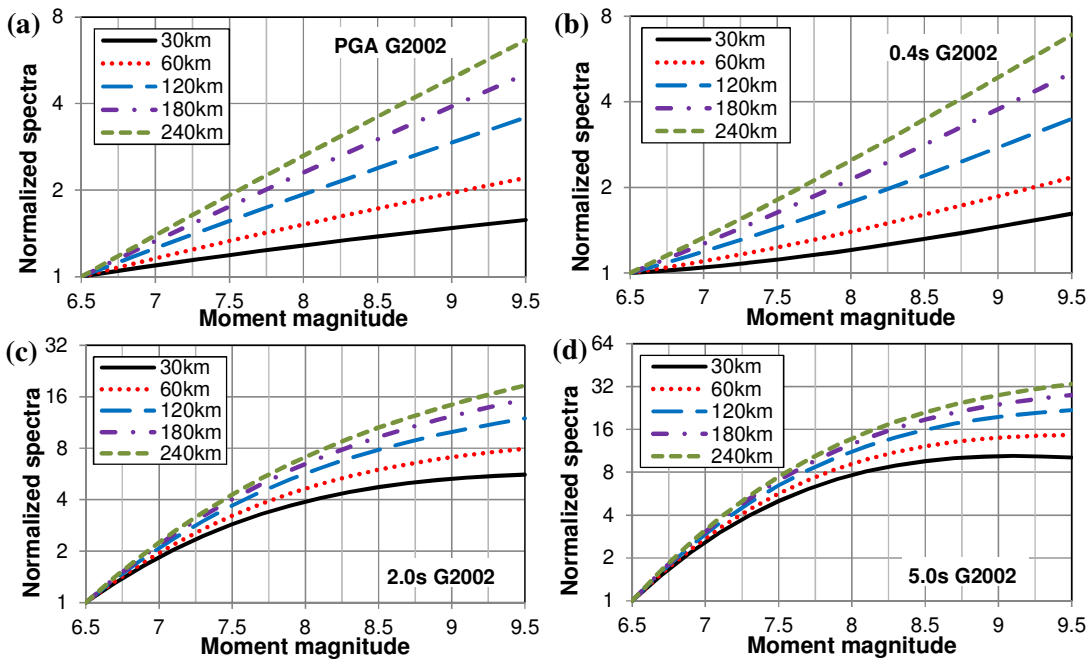


Figure 3 Normalized spectra predicted by the Gregor et al. 2002 model for (a) peak ground acceleration, (b) 0.4s, (c) 2 and (d) 5s spectral periods

Figure 3 shows the normalized spectra from the G2002 model for the same spectral periods and source distances. This model used a linear magnitude-dependent geometric attenuation term and has a constant added distance term to provide finite prediction at zero distance. A magnitude-cubed term was used to provide variable MSR with magnitude but the coefficient varies between negative and positive. The positive values produce an MSR increasing with increasing magnitude, which is not consistent with the models for crustal earthquakes reviewed by Zhao and Lu (2011) and two other models reviewed in the present study. Figure 3(a) shows that the normalized PGA is essentially a linear function of magnitude and the MSR increases with increasing source distance, an effect of the linear magnitude-dependent geometric attenuation function. The MSRs for PGA at all distances are much smaller than those of the Z2006 model. For example, at $M_w=9$, the normalized PGA at a source distance of 30km is only 1.5 times that from an $M_w=6.5$ event, while the same ratio from the Z2006 model is 4.7. The normalized spectra for an $M_w=9$ event are 1.9, 3, 3.9 and 4.9 at source distances of 60, 120, 180 and 240km, respectively, while the normalized spectra from the Z2006 model are 6.8, 10, 11 and 11.7 at the same distance, varying between 2.4 and 11.7 times those of the G2002 model. Figure 3(b) shows the normalized spectra at 0.4s spectral period for the G2002 model. The curvature of the normalized spectra is positive, in contrast to the other spectral periods and those of the Z2006 model. The increase in MSR with increasing magnitude is caused by the positive values for the magnitude-cubed term. The average MSRs are much less than those of the Z2006 model. At $M_w=9.0$, the normalized spectra vary between 1.5 and 5.2 in a distance range of 30-240km while the normalized spectra of the Z2006 model vary between 7.2 and 13. At 2s spectral period, the normalized spectra of the G2002 model in Figure 3(c) are still significantly lower than those of the Z2006 model shown in Figure 2(c). The normalized spectra from the G2002 model at 5s (Figure 3d) are very close to those of the Z2006 model shown in Figure 2(d). The normalized spectra are nearly constant for magnitude over 9 at a source distance of less than 30km at 5s spectral period.

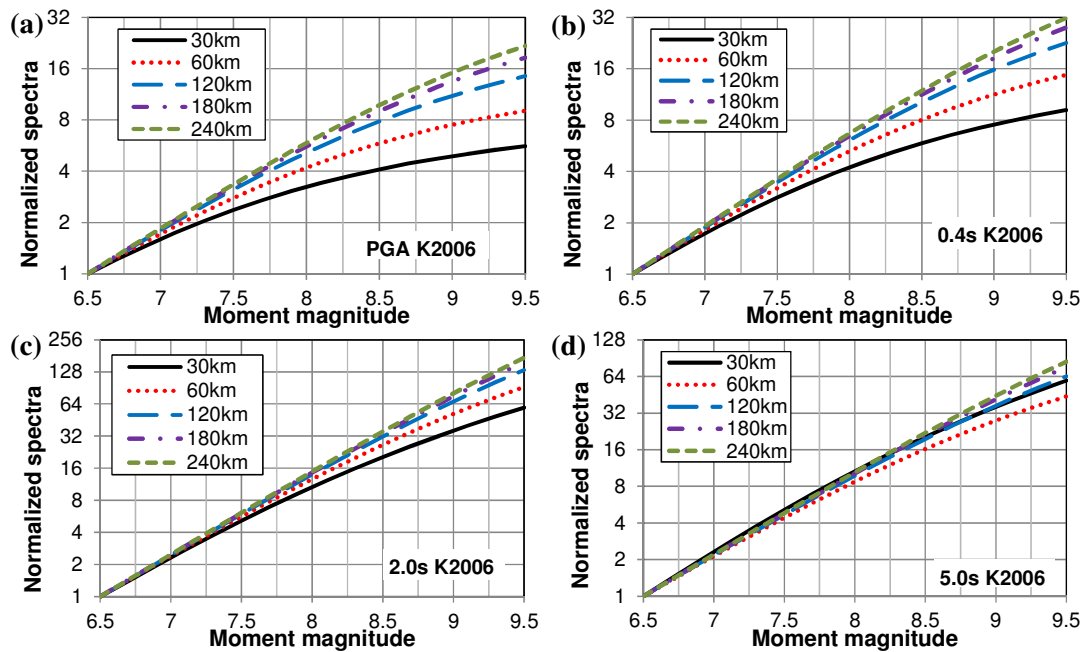


Figure 4 Normalized spectra predicted by the Kanno et al. 2006 model for (a) peak ground acceleration, (b) 0.4s, (c) 2s and (d) 5s spectral periods

Figure 4 shows the normalized spectra from the K2006 model. This model has very similar normalized PGA to that of the Z2006 model, and only moderately larger than that of the Z2006 model at a source distance of 180km or larger, as shown in Figure 4(a). Figure 4(b) shows the normalized spectra at 0.4s. They are similar to or slightly higher than those of the Z2006 model at distances equal to or less than 60km. At a large distance, the normalized spectra are about 1.5-1.8 times those of the Z2006 model at $M_w=9.0$. At long periods, compared with the results in Figures 2(c) and 2(d), the normalized spectra are much larger than those of the Z2006 model by a factor of up to 3, as shown in Figures 4(c) and 4(d). The normalized spectra increase almost linearly with increasing magnitude because the K2006 model does not have a magnitude-squared term at long periods.

The analyses presented here show a very large variation in the MSRs among the 3 models, and the differences are extremely large between the Z2006 and the K2006 models even though they were both derived from the Japanese data. The G2002 model has the lowest MSRs but the curvature of the normalized spectrum is positive for some spectral periods, suggesting that the normalized spectrum increases faster than the linear function of magnitude. That is not consistent with all other models evaluated here and in the study of Zhao and Lu (2011), and may not be physically plausible either. However, the small MSRs of the G2002 model at short

distance appear to lead to better prediction of the data from the 11 March 2011 ($M_W=9$) Japan earthquake than the other models compared by Boore (2011, personal communication).

METHOD OF ANALYSES

The objective of the present study is to assess the magnitude scaling rates (MSRs) for large subduction interface earthquakes. Zhao and Lu (2011) suggested that the use of a random effects model makes the analyses complicated, with interpretation required for both the magnitude term and the inter-event residuals. Also, the use of a magnitude term and the inter-event residuals means that the statistical power of the events that have only few records, for example, for 15 events that have fewer than 10 records, may be reduced significantly. To accommodate those events with a small number of records, the earthquakes are divided into 8 groups according to their magnitudes. The magnitude spread in each group is less than 0.2 magnitude units. The total number of records for PGA in each group varies between 28 and 536, so that each group of earthquakes has a reasonable number of records for statistical analyses. Each group of events can then be treated as an earthquake with a magnitude equal to the average magnitude of all events in this group. In the present study, all data are from Japan. The model parameters such as site class terms, depth terms and the terms that control the near-source model prediction from previous studies (e.g. Z2006; Zhao 2010), can be used, to avoid any effect from the reduced number of records compiled in the present study. The Zhao (2010) study accommodated the variation of geometric attenuation rates for both shallow crustal and subduction slab events, and depth-dependent anelastic attenuation rates for subduction interface events.

The model parameters from Zhao (2010) are used for site class and depth, and near-source terms. With the earthquakes grouped together according to their magnitude, and adopting the site class terms, depth terms and near-source terms, a very simple model can be used to assess the magnitude scaling for large subduction interface earthquakes from Japan.

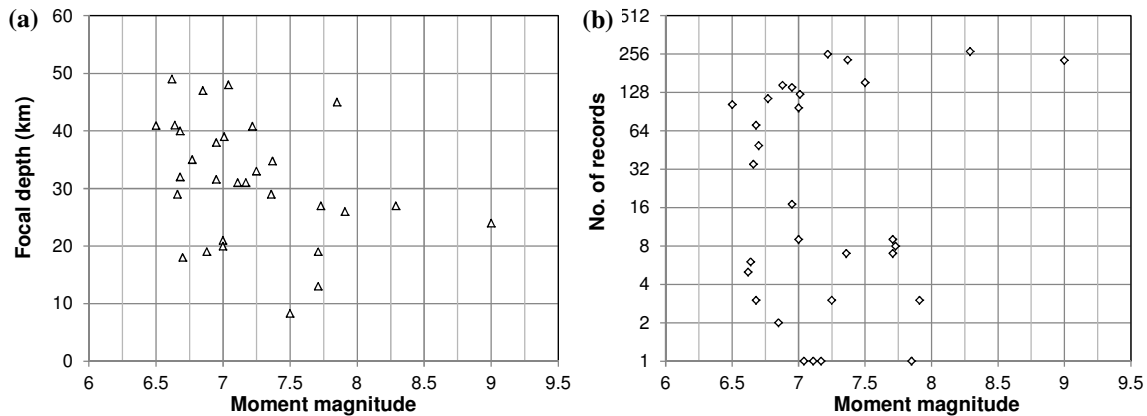


Figure 5 Distribution of strong-motion records from large subduction interface earthquakes from Japan, with respect to magnitude and focal depth in (a) and the number of records for each of the 30 earthquakes with a magnitude of 6.5 or larger, including 230 records from the 11 March 2011 earthquake with $M_W=9.0$, in (b)

STRONG-MOTION DATASET

2100 strong-motion records from 30 subduction interface earthquakes with a magnitude of 6.5 or larger were compiled, including 230 records from the recent 11 March 2011 $M_W=9.0$ earthquake (NIED 2011). The dataset has 256 records from the 26 September 2003 $M_W=8.3$ event, 153 records from the 9 March 2011 $M_W=7.5$ event, 222 records from the 26 September 2003 $M_W=7.4$ event, and 256 records from the 16 August 2005 $M_W=7.2$ event. The dataset also includes records from other large subduction interface events used in the Z2006 model. Figure 5(a) shows the earthquake distribution with respect to magnitude and focal depth, and Figure 5(b) shows the number of records for each event and its magnitude. Half of the events have 10 records or fewer and four events have only one record. Figure 6(a) shows the data distribution with respect to source distance and magnitude from SC I sites, and Figure 6(b) for records from SC II sites. Figure 6(c) shows the records from SC III sites and Figure 6(d) shows those from SC IV sites. The site classes were from Zhao et al. (2006b) and were broadly similar to those of NEPR site classes (BSSC 2000); see Table 1 in Zhao (2010). Fault rupture models are available for 20 of the 30 earthquakes and the hypocentral distances were used for the events without a fault rupture model.

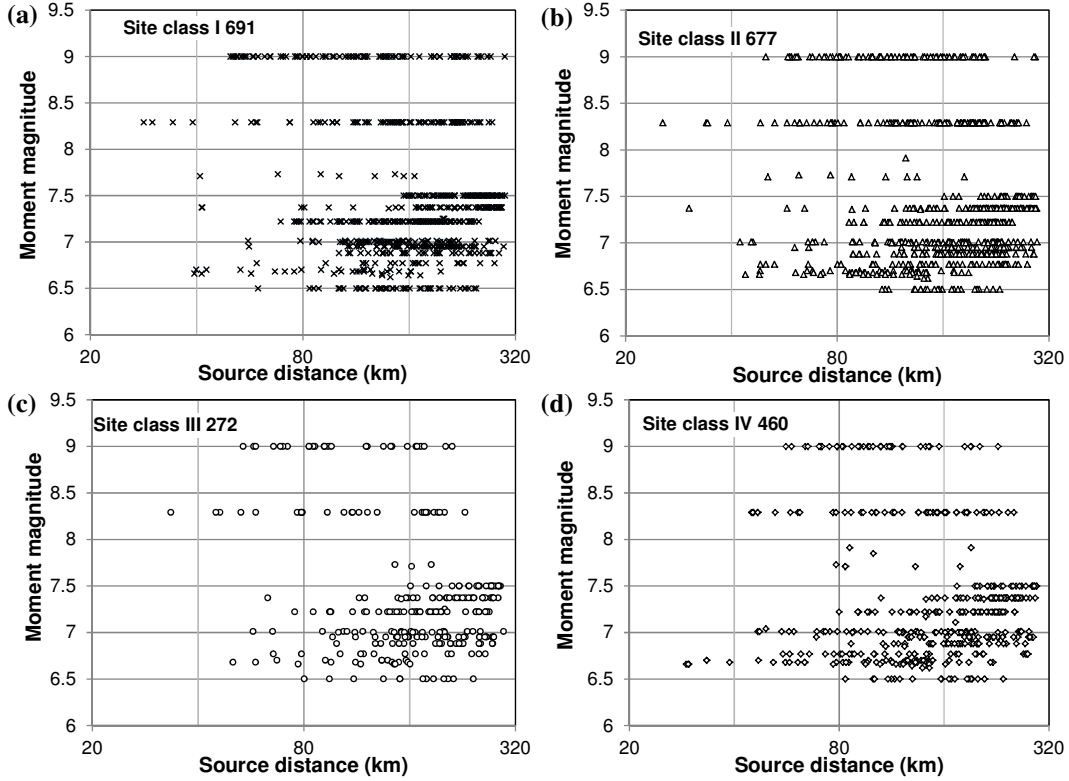


Figure 6 Distribution of strong-motion records with respect to distance and magnitude, (a) 691 records for site class I, (b) 677 records for site class II, (c) 272 records for site class III and (d) 460 records for site class IV

Figure 7 shows the attenuation of the normalized PGA and response spectra at 3 spectral periods and a few features can be observed. The PGA and acceleration spectra were normalized to SC II site class condition, at a focal depth of 20km using the site and the depth terms from the Z2006 model. Visual inspection suggests that the data from the $M_W=9$ and $M_W=8.3$ events are similar at distances over 150km. The PGA and spectral accelerations at 0.5s and 1.0s from the $M_W=9$ event are, on average, moderately larger than those from the $M_W=8.3$ and $M_W=7.5$ events at distances within 150km. The PGA and spectral accelerations at 0.5s and 1s from the $M_W=7.5$ and 8.3 can be fitted with an attenuation function without a magnitude term very well. At 5s, Figure 7(d) shows that the spectra from the two larger events are comparable while the spectra from the $M_W=7.5$ event are evidently smaller than those from the other two events. Figures 7(a) - 7(c) show that the attenuation rates within a distance of 170km are larger than those over 170km; this is especially obvious in Figure 7(b) for 0.5s. Linear scales were deliberately used for the distance in these plots, so that this feature would not be visually diminished by a logarithmic scale. This feature of the variation in attenuation rate with distance will be incorporated in the geometric attenuation rates, to avoid the use of a positive anelastic attenuation rate in order to achieve the best fit.

A SIMPLE ATTENUATION MODEL FOR ASSESSING MAGNITUDE SCALING

For subduction interface earthquakes, the anelastic attenuation rate for shallow events differs from that of deep events, as shown by Zhao (2010). First, the acceleration spectra were normalized to SC II site class and a focal depth of 20km using the results from the Zhao (2010) study. The normalization effectively deleted these parameters from the attenuation model. A simple model is proposed in the present study,

$$\log_e(y_{i,j}) = \alpha[\log_e(r_{i,j}) + \beta \log_e(x_{i,j} + r_a)] + b_{SH} x_{i,j} \delta_{SH} + b_{DEEP} x_{i,j} \delta_{DEEP} + \gamma_i \quad (1)$$

$$\delta_{i,k} = \begin{cases} 1 & \text{if } k = i \\ 0 & \text{if } k \neq i \end{cases} \quad \delta_{SH} = \begin{cases} 1 & \text{if depth} \leq 25 \text{ km} \\ 0 & \text{if depth} > 25 \text{ km} \end{cases} \quad \delta_{DEEP} = \begin{cases} 1 & \text{if depth} > 25 \text{ km} \\ 0 & \text{if depth} \leq 25 \text{ km} \end{cases} \quad \psi_i = \begin{cases} M_i & \text{if } M_i \leq C_{\max} \\ C_{\max} & \text{if } M_i > C_{\max} \end{cases} \quad (2a,b,c,d)$$

$$r_{i,j} = x_{i,j} + \exp(c + d\psi_i) \quad (3)$$

where x_i is the shortest distance between a recording station and the fault plane, and N_m is the total number of earthquake groups. Coefficient α is the geometric attenuation rate, b_{SH} is the anelastic attenuation rate for earthquakes with a focal depth of 25km or less, b_{DEEP} is the anelastic attenuation rate for earthquakes with a focal depth over 25km, and γ_i is a constant for the i^{th} group events.

Parameter β is the added geometric attenuation rate primarily for records with a source distance larger than r_a as used by Chiou and Youngs (2008) and Zhao and Lu (2011) to accommodate the reduced attenuation rate at large distances as shown in Figure 7. Subscript i denotes the i^{th} earthquake group and j denotes the j^{th} record in the i^{th} earthquake group. The terms c and d control the near-source prediction, and the values from the Zhao (2010) model were adopted, as these terms cannot be determined reliably from the present dataset. For large and great earthquakes, C_{max} is used to adjust the model prediction within about 50km. The main interest in the present study is to determine the constant γ_i for each earthquake group, and the MSR can then be assessed by the variation of γ_i with the average magnitude for each earthquake group.

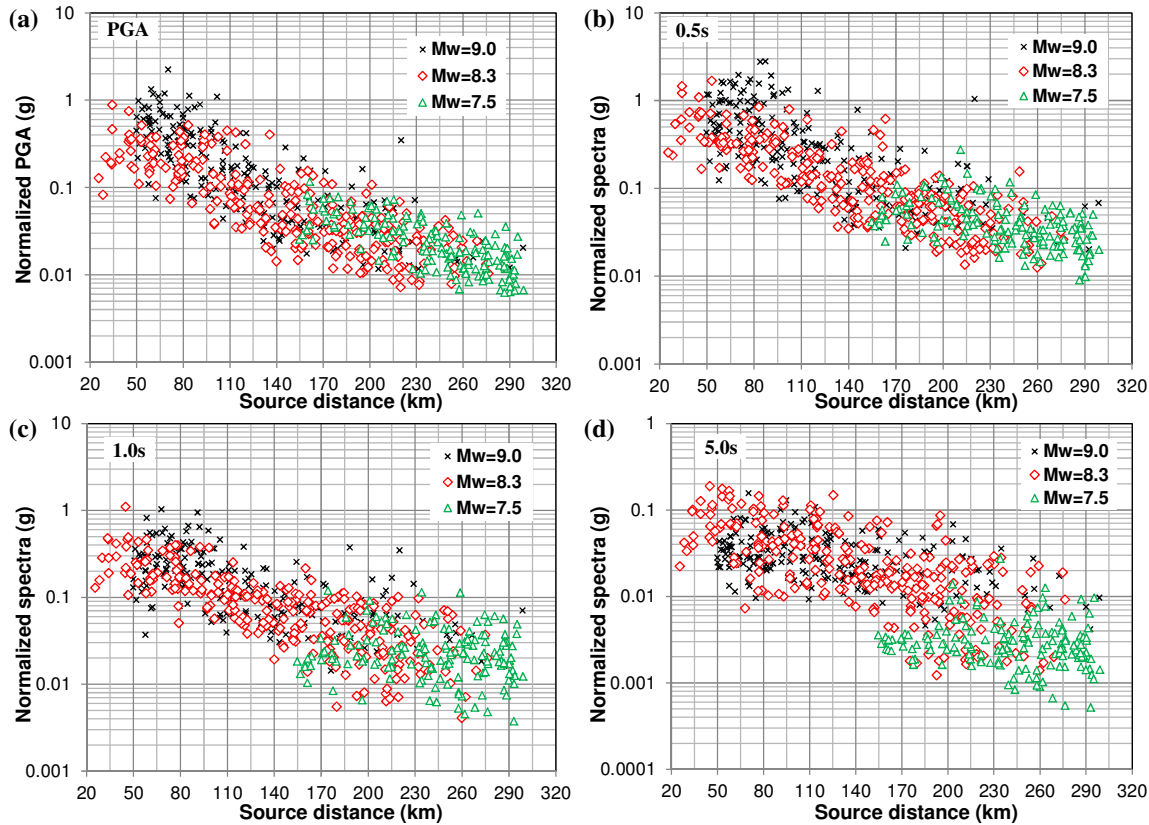


Figure 7 The attenuation of normalized spectra with respect to source distance (the closest distance to the fault rupture plane) for the two large events and hypocentral distance for the other earthquake, (a) PGA; and (b) spectra at 0.5s; (c) at 1s and (d) at 5s. The PGA and spectrum were normalized to site class II, i.e. multiplied by $\exp(S_k - S_2)$ where S_k and S_2 are the site terms of the Z2006 model for the k^{th} class and the 2nd class, respectively

The total number of terms to be determined in Equation (1) is 16, which is moderately large and some may not be statistically significant. As the total number of records and the number of records in each earthquake group are reasonably large, it is possible to rely on statistical properties of each term to determine which parameter is statistically “necessary”, especially the constants for each group of earthquakes. The approach was to perform a regression analysis assuming all the terms in Equation (1) were non-zero, and the t -test was carried out for each term to verify that the estimate for each term was statistically significant at a 5% significance level. Ratios of the median estimates for each term over their standard deviations were computed. The term with the smallest ratio and that was not statistically significant was deleted. This process was repeated until the estimates for all terms in the final model were statistically significant. Parameter β was obtained by minimizing model prediction error subjected to obtaining negative or zero values for all anelastic attenuation terms.

MAGNITUDE SCALING

Next, the constants for each group of earthquakes in Equation (1) are presented. These constants represent the effect of earthquake magnitude for each group of events rather than each event. However, the difference in magnitude over the events in one group is less than 0.2 magnitude unit, and each magnitude group can be taken as “one event”. A function of magnitude that can be fitted to these constants very well can be taken as the “magnitude scaling part” in an attenuation model. Thus, the MSR is the slope of a curve in the 2-D plot of the constants in Equation 1 versus the average magnitude. Because the interest of the present study is to assess the

magnitude scaling for large subduction interface earthquakes, normalization can be used to present the possible magnitude scaling so as to eliminate the effect of the absolute values. Figures 8-10 present the constant γ_k in Equation (1) minus the constant γ for $M_w=6.5$. The differences between the constants for a given group of earthquakes and that for the $M_w=6.5$ group are labelled as normalized magnitude scaling in a natural logarithm scale, and this function of the magnitude may be used in an attenuation model. For the models used by Youngs et al. (1997) (referred to as Y1997), and the Z2006, K2006 and Zhao (2010) studies, the exponential of the magnitude scaling presented in Figures 8-10 represents the normalized spectrum at a very large distance, as shown in Figures 2-4.

A number of functions can be fitted to the normalized spectrum. The data suggest that the simplest one would be to fit a straight line to the data for magnitude over 7 and the slope of the straight line would be the magnitude term that can be used in an attenuation model for the earthquakes over magnitude 7. The slopes are labelled as MSR in Figures 8-10. Another possibility is to fit a bilinear model with two segments and the slope of the second segment (for magnitude larger than the corner magnitude) can be used as the magnitude term in an attenuation model for large earthquakes. The slope for the first segment would be the magnitude term for events with a magnitude between 6.5 and the corner magnitude. The distribution of the constants with respect to magnitude shown in Figures 8-10 strongly supports a bilinear model for all periods. The third possible option is to fit a smoothed curve to the data. The functions used in Figures 8-10 have the following form,

$$F(M_w) = (M_w - 6.5)\text{Exp}[\mu \log_e(M_w - 6.5 + \rho) + \varphi] \quad (4)$$

where μ , φ and ρ are constants to be determined by a regression analysis. Equation (4) is not overly complex to use for an attenuation model. The curved magnitude scaling fits the data even better than a bilinear model.

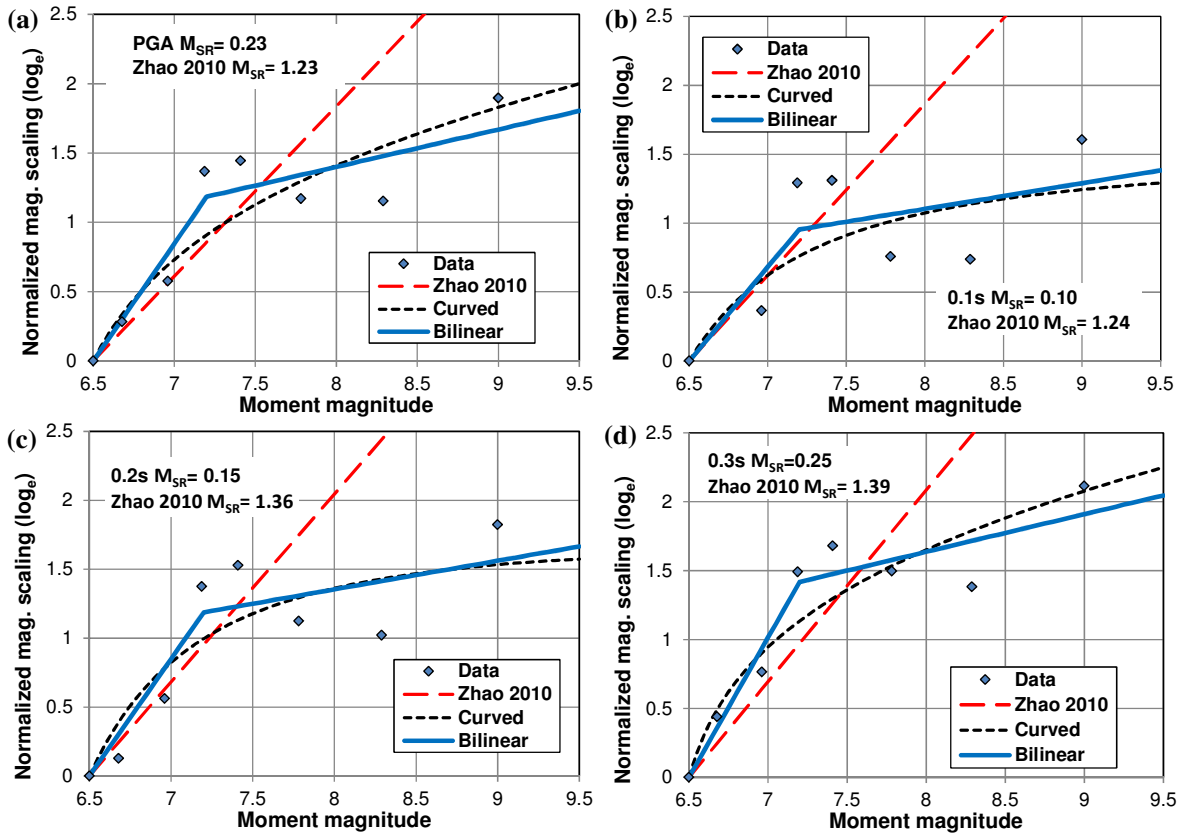


Figure 8 Normalized magnitude scaling in natural logarithm scale as a function of moment magnitude, a possible magnitude scaling rate (MSR, the slope of the fitted straight line function of magnitude for earthquakes with a magnitude 7 or larger), a bilinear model and a curved model fitted to the data, for (a) 0s (PGA), (b) 0.1s, (c) 0.2s and (d) 0.3s spectral periods. The curved model is given in Equation (4)

Figure 8 shows the normalized magnitude scaling for PGA, and spectra at 0.1, 0.2 and 0.3s spectral periods together with those derived from Zhao (2010) (broken line), the bilinear model, the curved model in Equation (4) and the MSR derived from a straight line fitted to the data from earthquakes over $M_w=7$. The scatter is large but generally smaller than or similar to the inter-event standard deviation for large events in the Zhao (2010) model. The MSR from the bilinear model and the linear model for events

$M_w > 7$ are generally similar, but they are much smaller than those of all attenuation models for subduction interface events examined in the present study. For example, for PGA, the MSR is 1.23 in the Zhao (2010) model. The linear model gives an MSR varying between 0.10 at 0.1s and 0.25 at 0.3s while the MSR for the Zhao (2010) model vary between 1.23 and 1.39. The corner magnitudes that separate two linear segments of the bilinear models are 7.2 for the data in Figure 11. The curved models provide better fitting to the data.

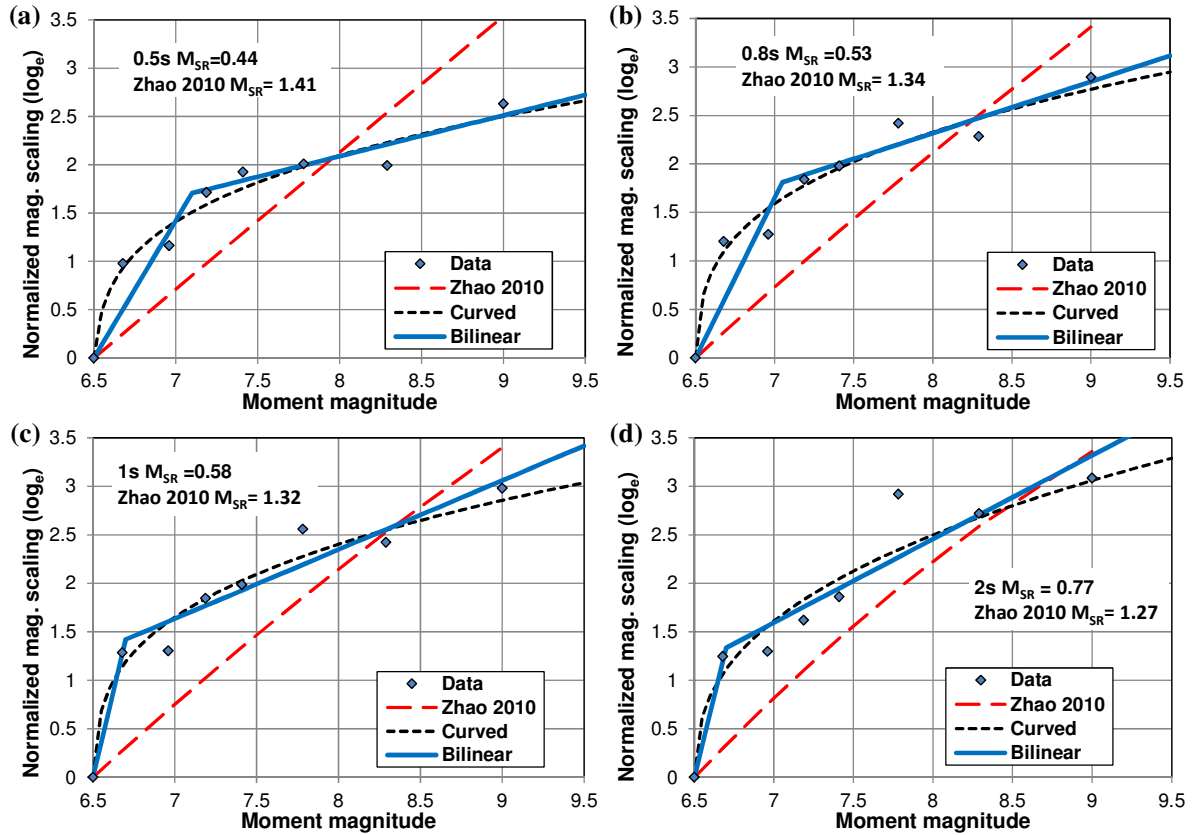


Figure 9 Normalized spectra in natural logarithm scale $f(m)$ as a function of moment magnitude, a possible MSR (the slope of the fitted straight line function of magnitude for earthquakes with a magnitude 7 or larger), for (a) 0.5s, (b) 0.8s, (c) 1s and (d) 2s spectral periods. The curved model is given in Equation (4).

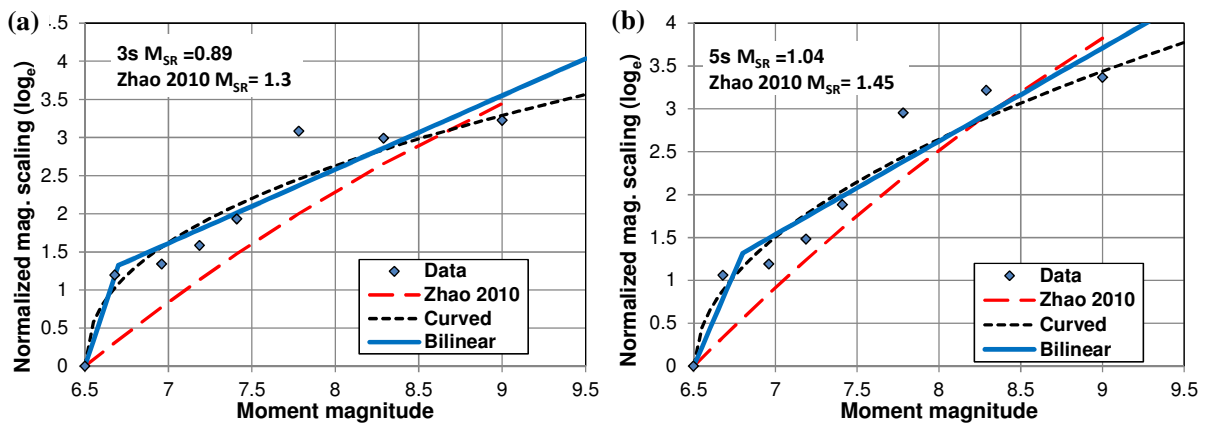


Figure 10 Normalized spectra in natural logarithm scale $f(m)$ as a function of moment magnitude, a possible MSR (the slope of the fitted straight line function of magnitude for earthquakes with a magnitude 7 or larger), for (a) 3s and (b) 5s spectral periods. The curved model is given in Equation (4).

Figure 9 presents the normalized magnitude scaling for spectra at 0.5s, 0.8s, 1s and 2s. The MSR derived from the linear model increase with increasing spectral period, from 0.44 at 0.5s to 0.77 at 2s. Again the MSR derived from the linear model are generally

similar to the slope of the second segment for events larger than 7. The MSR for the Zhao (2010) model derived from the broken lines in Figure 9 are 1.41 at 0.5s, 1.34 at 0.8s, 1.32 at 1s and 1.27 at 2s, about 2.5 times those for the linear models. Note that the magnitude-squared term is less than zero at spectral periods over 0.15s and the absolute values increase from 0 at 0.1s to 0.16 at 5s. When the magnitude-squared term is not zero, the MSR is computed for an $M_w=8$ event.

Figure 10 shows the normalized magnitude scaling for 3s and 4s spectral periods. The MSR from a linear model is 0.89 for 3s and 1.04 for 5s while the Zhao (2010) model has an MSR of 1.3 at 3s period and 1.45 at 5s. The MSR of the bilinear model for large events are similar at both spectral periods.

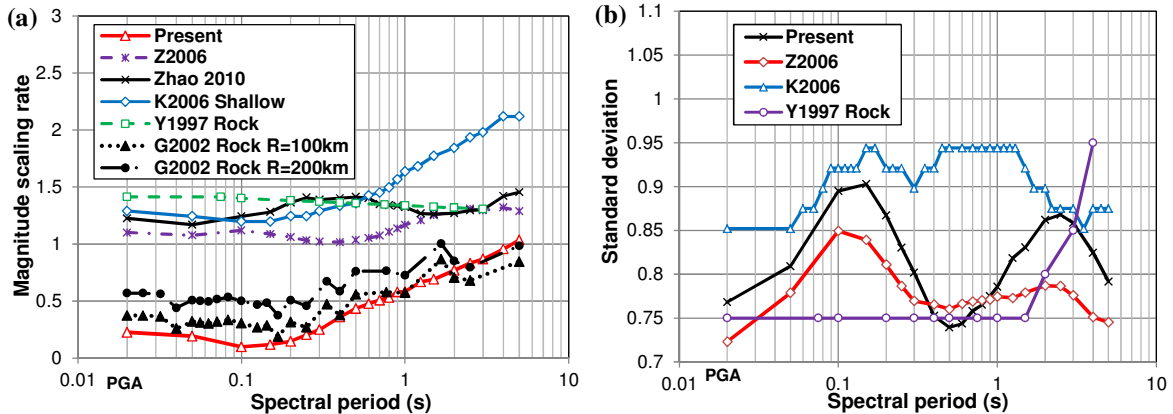


Figure 11 Comparison of MSR at large distance derived from the present study with those from the Z2006 and Zhao (2010) models, the K2006 model for shallow earthquakes, the Youngs et al. (1997) model for rock sites and the G2002 model for rock sites in (a), and comparison for the standard deviation for the model derived in the present study with those from the Z2006 model, the K2006 model for shallow earthquakes and the Youngs et al. 1997 model for rock sites in (b)

Figure 11(a) compares the MSR of the present study with those of various models. Note that the G2002 model has a magnitude-dependent geometric spreading term and the MSR depends on source distance. Figure 11(a) presents the MSR computed for 100km and 200km source distances for the G2002 model while the MSR for all other models are for large distances where the magnitude-dependent added distance has little effect. The Y1997, Z2006 and Zhao (2010) models all have magnitude-squared or cubed terms and the MSR was computed at $M_w=8$. The MSR from the G2002 model for rock sites at a source distance of 100km are very close to those of the present study. However, at source distance of 30km, the MSR of the G2002 model are less than those from the present study. The MSR from the Z2006, Zhao 2010 and Y1997 models vary between 1.0 and 1.5 at all periods. The magnitude-scaling rates of the K2006 model are similar to those of the Z2006 model at periods up to 0.8s and then increase quickly with increasing period, with the largest value being just over 2.

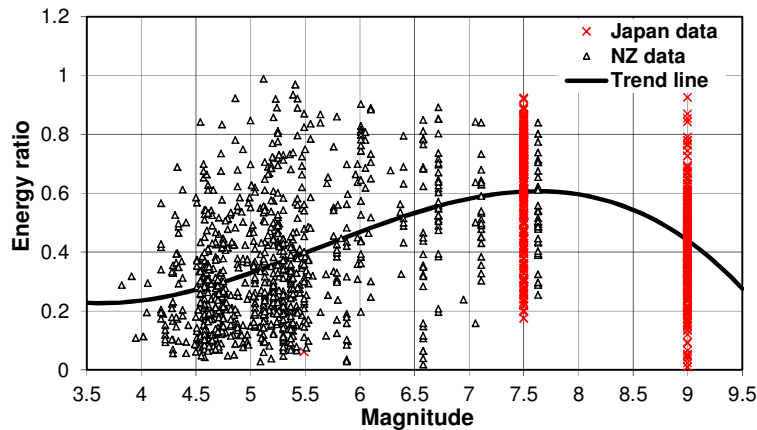


Figure 12 Energy ratios calculated according to Zhao and Lu (2011) for 5s spectral period for the data from New Zealand and two recent large earthquakes from Japan.

Zhao and Lu (2011) suggested that the reduced magnitude scaling rate for large earthquakes was a result of reduced energy ratio (the ratio of energy contributed to the response spectrum at a given spectral period over the total energy) for large earthquakes. Figure 12 shows the energy ratios for a set of strong-strong-motion records from New Zealand and those from the two large subduction

earthquakes ($M_w=7.5$, 9 March 2011 and $M_w=9$, 11 March 2011). Figure 12 shows clearly that the average energy ratio for the $M_w=9$ event is considerably smaller than those for the earthquakes with a magnitude of 7-7.5.

DISCUSSIONS AND CONCLUSIONS

Using a similar method to a previous study by Zhao and Lu (2011), the present study investigates magnitude scaling for large subduction interface earthquakes from the Zhao et al. (2006a) (referred to as Z2006) model, Kanno et al. (2006) (referred to as K2006) model and Gregor et al. (2002) (referred to as G2002) model. Similar to the models for large shallow crustal earthquakes, the magnitude-scaling rates (MSRs) from the models for subduction interface earthquakes vary significantly among different models. The difference between the Z2006 and K2006 models at periods over 1s is alarmingly large, as the two models were both derived from the Japanese data.

2100 strong-motion records from 30 large subduction interface earthquakes in Japan with a moment magnitude of 6.5 or larger were compiled, including the 11 March 2011 $M_w=9$ event. The strong-motion records were then normalized by the site and the depth terms from the Zhao (2010) study, and therefore the site condition and focal depth are no longer required for a new model investigated in the present study. In order to use the small number of records from an event with a large magnitude, the earthquakes were grouped together according to their magnitudes. Each of the eight groups has earthquakes with a magnitude difference within 0.2 magnitude unit and the smallest number of records in each group is 28. Each group was treated as “one” event and the average magnitude of each group was used as its magnitude.

An attenuation model with geometric and anelastic attenuation rates and a constant term for each earthquake group was fitted to the normalized spectra. The geometric attenuation rate contains a term that allows variation of geometric attenuation rate along the source distance to accommodate the observed attenuation characteristics of the data. The simple model also allows for a depth-dependent anelastic attenuation rate as suggested by the Zhao (2010) study. The simple model without a magnitude term allows a constant term for each earthquake group to account for the magnitude effect. Three possible models were used to derive the magnitude scaling rates – a simple linear model for those events with a magnitude over 7 supported by the data, a bilinear model with a corner magnitude to separate the magnitude scaling function into two linear segments and a simple curved model as a function of magnitude. These functional forms can be used in an attenuation model directly with the parameters determined by regression analyses on a complete dataset. The slopes of these straight lines would be the simple magnitude terms for a new model, while the interest of the present study is primarily to assess the magnitude-scaling rate (MSR) – the slope magnitude scaling curves for large earthquakes.

The results show that MSRs derived from large subduction interface earthquakes are significantly smaller than those of the empirical prediction equations derived from real earthquake records. At short periods, the MSRs derived in the present study are only a fraction of those from the three empirical attenuation models, derived from primarily the Japanese data. At spectral periods over 0.5s, the MSRs derived in the present study are between about 1/3 and 1/2 of those from the existing empirical models. The MSRs of the G2002 model, derived from synthetic data using a stochastic finite-fault model, are surprisingly close to the values derived from the data in the present study, especially at short distances. However, at a distance of 50km the MSRs of the G2002 model are less than the values from the present study.

The results of the present study, however, differ from those of the Zhao and Lu (2011) study for shallow crustal earthquakes. Zhao and Lu (2011) showed that a zero magnitude-scaling model worked well for the data from 13 large crustal earthquakes with M_w over 7 for spectral periods between 0.6 and 5s, while the present study shows that the MSR increases with increasing spectral period. While no theoretical justification can be provided to explain the difference, the anelastic attenuation rates for a deep subduction interface event are considerably smaller than those from shallow subduction interface events and shallow crustal events. This means that the seismic waves from a distant part of the fault for a deep subduction earthquake are attenuated much less rapidly than for those from a crustal event, allowing a large part of the ground-motion generation area to produce the seismic waves that contribute significantly to the response spectrum at a recording station. This leads to a larger magnitude beyond which ground-motion amplitude would be saturated in the period range for engineering applications. 20 of the 30 events used in the present study have a focal depth larger than 25km, the boundary between shallow and deep subduction interface earthquakes assigned in the Zhao (2010) study.

Another feature of the subduction interface earthquake is that its fault area can have a width that can be very close to its length. This may allow a larger ground-motion generation area on a fault to produce ground motions that contribute to the response spectra at a station for a given distance, compared with a relatively narrow and long fault for a crustal earthquake.

It is encouraging to find that numerical simulations used by Gregor et al. (2002) produced very similar magnitude scaling to those derived from the present study. The good match may allow researchers to apply this method to fill in the data gap and/or to constrain the model prediction for large damaging subduction earthquakes. The recent study by Atkinson and Goda (2010) shows that the synthetic strong-motion records generated by a stochastic finite-fault model developed by Motazedian and Atkinson (2005) produced

very similar inelastic response spectra to those of real strong-motion records with minor modification or amplitude scaling. These results provide confidence in using synthetic strong-motion records for engineering applications.

ACKNOWLEDGEMENT

The author wishes to thank Dr. David Rhoades for his review of the manuscript and Jane Forsyth for her editorial comments. The work reported here is partially supported by New Zealand Foundation for Science and Technology: New Zealand Hazards Platform contract C05X0907.

REFERENCES

- Abrahamson, N. A. and W. J. Silva [2008]. Summary of the Abrahamson & Silva NGA Ground-Motion Relations, *Earthquake Spectra* Vol. 24, No 1, pp. 67-97
- Atkinson, G.M. and D.M. Boore [2003]. Empirical Ground-Motion Relations for Subduction-Zone Earthquakes and Their Application to Cascadia and Other Regions *Bull. Seismol. Soc. Am.* Vol. 93, pp. 1703 - 1729.
- Atkinson, G.M. and K. Goda [2010]. Inelastic Seismic Demand of Real versus Simulated Ground-Motion Records for Cascadia Subduction Earthquakes, *Bull. Seismol. Soc. Am.* Vol. 100, pp. 102–115
- Boore, D.M. and G.M. Atkinson [2008]. Ground-Motion Prediction Equations for the Average Horizontal Component of PGA, PGV, and 5%-Damped PSA at Spectral Periods between 0.01 s and 10.0 s, *Earthquake Spectra*, Vol. 24, No 1, pp. 99-138
- Building Seismic Safety Council (BSSC) [2000]. The 2000 NEHRP Recommended Provisions for New Buildings and Other Structures, Part I (Provisions) and Part II (Commentary), FEMA 368/369, Washington DC
- Campbell, K.W. and Y. Bozorgnia [2008]. NGA Ground Motion Model for the Geometric Mean Horizontal Component of PGA, PGV, PGD and 5% Damped Linear Elastic Response Spectra for Periods Ranging from 0.01 to 10s, *Earthquake Spectra*, Vol. 24, No 1, pp. 139-171
- Chiou, B. S.-J., and R.R. Youngs [2008]. An NGA model for the average of horizontal component of peak ground motion and response spectra, *Earthquake Spectra*, Vol. 24, No 1, pp. 173-216
- Gregor, N.J., W.J. Silva, I.G. Wong, and R.R. Youngs [2002]. Ground-Motion Attenuation Relationships for Cascadia Subduction Zone Megathrust Earthquakes Based on a Stochastic Finite-Fault Model, *Bull. Seismol. Soc. Am.* 92, 1923–1932
- Kanno T., A. Narita, N. Morikawa, H. Fujiwara, and Y. Fukushima [2006]. A New Attenuation Relation for Strong Ground Motion in Japan Based on Recorded Data, *Bull. Seismol. Soc. Am.* Vol. 96, pp. 879–897
- Motazedian, D., and G. M. Atkinson [2005]. Stochastic finite-fault modelling based on a dynamic corner frequency, *Bull. Seismol. Soc. Am.* Vol. 95, pp. 995–1010.
- NIED [2011]. http://www.k-net.bosai.go.jp/k-net/topics/TohokuTaiheiyo20110311/nied_kyoshin2e.pdf (last access date 29 April 2011)
- Silva, W., R. Darragh, C. Stark, I. Wong, J. Stepp, J. Schneider, and S. Chiou [1990]. A methodology to estimate design response spectra in the near-source region of large earthquakes using the Band-Limited-White-Noise ground motion model, in *Proc. Fourth U.S. National Conference on Earthquake Engineering*, Vol. 1, 487–494
- Youngs, R. R., S. J. Chiou, W. J. Silva, and J. R. Humphrey [1997]. Strong ground motion attenuation relationships for subduction zone earthquakes, *Seism. Res. Lett.* 68, 58–73.
- Zhao, J. X., J. Zhang, A. Asano, Y. Ohno, T. Oouchi, T. Takahashi, H. Ogawa, K. Irikura, H. K. Thio, P. G. Somerville, Yasuhiro Fukushima, and Yoshimitsu Fukushima [2006a]. Attenuation relations of strong ground motion in Japan using site classification based on predominant period, *Bull. Seismol. Soc. Am.* Vol. 96, No. 3, pp.898–913.
- Zhao, J. X., K. Irikura, J. Zhang, Y. Fukushima, P. G. Somerville, A. Asano, Y. Ohno, T. Oouchi, T. Takahashi, and H. Ogawa [2006b]. An empirical site classification method for strong motion stations in Japan using H/V response spectrum ratio, *Bull. Seismol. Soc. Am.* Vol. 96, No. 3, pp. 914–925.
- Zhao, J. X. [2010]. Geometric spreading functions and modelling of volcanic zones for strong-motion attenuation models derived from records in Japan, *Bull. Seismol. Soc. Am.* Vol. 100, No. 2, pp. 712–732
- Zhao, J.X., and M. Lu [2011]. Magnitude-scaling rate in ground-motion prediction equations for response spectra from large shallow crustal earthquakes, accepted for publication, *Bull. Seismol. Soc. Am.*